A Novel Approach for Invasive Weeds and Vegetation Surveys Using UAS and Artificial Intelligence

Conference Paper · August 2018

DOI: 10.1109/MMAR.2018.8485874

2 authors:

Juan Sandino
Queensland University of Technology
12 PUBLICATIONS **136** CITATIONS
SEE PROFILE

Luis Felipe Gonzalez
Queensland University of Technology
172 PUBLICATIONS **2,787** CITATIONS
SEE PROFILE

A Novel Approach for Invasive Weeds and Vegetation Surveys using UAS and Artificial Intelligence

Juan Sandino
Institute for Future Environments
Queensland University of Technology
Brisbane City, QLD 4000, Australia
Email: sandinoj@qut.edu.au

Felipe Gonzalez
Robotics and Autonomous Systems
Queensland University of Technology
Brisbane City, QLD 4000, Australia
Email: felipe.gonzalez@qut.edu.au

***Abstract*—Surveillance tasks of weeds and vegetation in arid lands is a complex, difficult and time-consuming task. In this article we present a framework to detect and map invasive grasses, combining UAVs and high-resolution RGB technologies and machine learning for data processing. This approach is illustrated by segmenting Buffel Grass (*Cenchrus ciliaris*) and Spinifex (*Triodia* sp.). Segmentation results produced individual detection rates of 97% for buffel grass, 96% for spinifex and 97% for the overall classification task. The algorithm is robust against variations in illumination, occlusion, object rotation and density of vegetation.**

***Index Terms*—biosecurity, *Cenchrus ciliaris*, drones, remote sensing, *Triodia* sp., UAV, vegetation assessments, weeds.**

I. Introduction

For the last decades, the effects of invasive grasses have resulted in catastrophic damages on host ecosystems worldwide. Attempts to control introduced plants have been remarkably complex owing to limited and challenging access to isolated regions, high operational expenses and, to a certain degree, the difficulty in campaigns for data collection campaigns [1]. invasive grasses have flourished in arid landscapes like Australia because of their resistance under hot, wet and dry conditions [2], [3]. Many species have invaded wetter and more fertile country areas and influenced the existence of endemic plant and animal populations [4]–[6]. Straightaway, efficient and reliable examination techniques are wanted to quantify development rates and directions of invasive grasses. [6]–[10].

The design and path planning of UAV systems together with the lower cost of off-the-shelf autopilots and affordable solutions [11]–[14], UAVs have seen a remarkable uptake on remote sensing approaches for invasive grasses and other vegetation surveillance [15]–[18]. Hyperspectral sensors to detect invasive grasses has shown breakthroughs over traditional methods like satellite imagery [19]. Some research present approaches that comprise UAVs and multispectral cameras for invasive plant mapping, obtaining detection rates up to 96% [20]–[23]. Nevertheless, several applications and ecologists still support the feasibility of using simpler UAVs and RGB cameras, with accurate results [24].

Data processing methods that evaluate and track vegetation have also offered diverse results. Amongst them, the calculation of vegetation and soil indexes for weed detection has achieved considerable demand [25]–[27]. Overall, supervised and unsupervised classification and segmentation algorithms are hugely affected by image quality, the number of spectral bands and spatial resolution or Ground Sampling Distance (GSD). Universal standards have not been determined by choosing adequate data processing and sensing technology processes that meet any application requirement [28]. This work presents an overview of the primary outcomes of the Plant Biosecurity CRC 2164 project "Developing pest risk models of Buffel Grass using Unmanned Aerial Systems and statistical methods" [29] and related publications [30]–[32]. It comprises UAVs, high-resolution RGB sensors and artificial intelligence to detect and map invasive grasses and other vegetation using a flexible survey method. This approach is represented through the automatic classification of buffel grass (*Cenchrus ciliaris*) and spinifex (*Triodia* sp.) in arid lands of Western Australia (WA).

II. Methodology

A. Framework

We designed a framework that comprises "Acquisition", "Preprocessing" , "Training", and "Prediction" stages, as depicted in Figure 1. First, High-resolution RGB imagery are acquired using a data collection campaign with a UAV. The photos are extracted and preprocessed to obtain samples with essential features. Moreover, those images are labelled and processed in a machine learning supervised classifier, which is fitted and optimised subsequently. Lastly, the orthomosaic image is completely processed to map the predicted locations of invasive grasses in the studied area.

B. Site

Methods are demonstrated in a case study located at the Cape Range National Park (CRNP), WA, Australia. The area includes mixed regions with buffel grass, decomposed vegetation, spinifex, arid and semi-arid soil, and other bushes. Photos

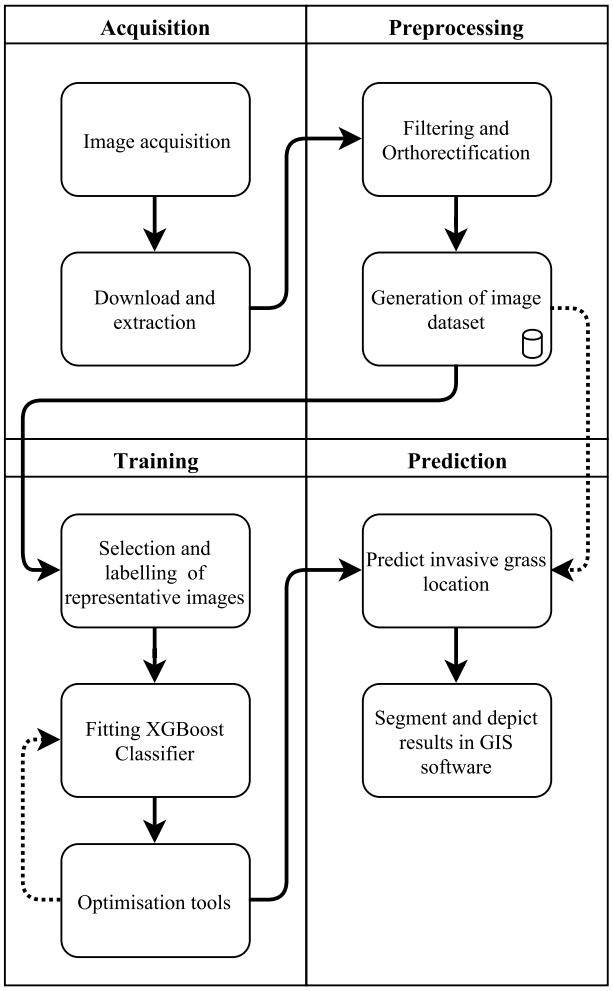

Fig. 1. Framework for detection of invasive grasses.

were captured in a continuous set of four flight campaigns. The mission was performed in July 10, 2016, from 12:30 to 14:30. Recorded weather conditions describe a sunny day, relative humidity of 46%, with south-easterly winds ranging from 17 to 26 km/h, a mean temperature of 21.2 °C, and no rainfall [33].

C. Drone and Flight Campaign

We used A Hexa-rotor DJI S800 EVO UAV (DJI, Guangdong, China) which followed a mission route using the DJI Ground Station 4.0 software solution. The mission was conducted at 66.9 ± 4.6 m altitude, 80% overlap, 50% side lap, a 6.6 km track distance at 16 km/h, and 1.0152 cm/pixel vertical and horizontal GSD. The drone specifications include brushless motors of high-performance, a whole weight of 4 kg, an incorporated gimbal that provides 3-axis active stabilisation of the utilised payload, and dimensions of 118 cm × 100 cm × 50 cm.

D. Camera

A Canon EOS 5DsR (Canon Inc., Tokyo, Japan) digital camera was used to acquire high-resolution pictures. The

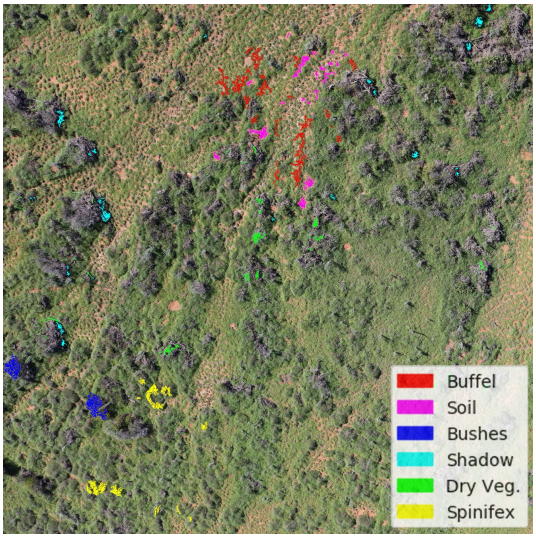

Fig. 2. Image with highlighted blobs using distinct colours.

camera has an image resolution of 50 MP, a focal length of 28 mm, a speed "ISO-400", image sensor size of 36 × 24 mm, an exposure time of 625 µs, and a GPS sensor.

E. Software tools

An orthomosaic image was first obtained by processing more than 500 raw photos with Agisoft PhotoScan 1.3. The software produced a stitched picture of 44800 × 17200 pixels, which sized 2.4 GB. This image was consequently split into 4816 frames of 400 × 400 pixels in TIF and KML image formats. Then, several samples of cropped regions from the orthophoto were also derived to be labelled through GIMP 2.8.22, and fit a supervised classifier. The imagery was processed in Python 2.7.14 and Scikit-learn 0.19.1 [34], XGBoost 0.6 [35], Matplotlib 2.1.0 [36] and OpenCV 3.3.0 [37] third-party libraries.

F. Labelling of imagery

Owing to the diverse conditions where invasive grasses are found in CRNP, 11 pictures were picked and examined by experts applying photo interpretation. Buffel Grass and spinifex as invasive grasses and specific objects in the area were marked using distinct colours as shown in Figure 2.

Picture labelling is done using a mask for each sample. The mask is created by following Equation 1, which assigns integer values for all the marked pixels.

$$H_{(x,y)} = \begin{cases} a & \text{if } S_{(x,y)} = F_{(R,G,B)} \\ 0 & \text{otherwise} \end{cases} \quad (1)$$

where H is the mask for each sample S and a is an integer number that identifies the depicted colour in $F_{(R,G,B)}$. For this case study, we assigned a following the list: 1: buffel grass, 2: soil; 3: bushes; 4: shadows; 5: decomposed vegetation; 6: spinifex.

Algorithm 1 Segmentation of invasive grasses.

Needed: orthomosaic picture I. Set of samples G. Set of masks H

Training

1: **for** $i \leftarrow 1, n$ **do**
2: Load G_i and H_i photos
3: Transform colour model of G_i to HSV
4: Add each colour channel to the feature array D
5: Apply 2D filters on G_i and add their results into D
6: From G_i and H_i, filter only the labelled pixels on D
7: **end for**
8: Divide D into a training data D_T and testing data D_E
9: Fit a XGBoost classifier X using D_T
10: Apply K-fold cross validation with D_E
11: Apply grid search using parameters of X

Segmentation

12: **for** $i \leftarrow 1, m$ **do**
13: Load I_i photo
14: Transform colour model of I_i to HSV
15: Predict the object using X
16: $O_i \leftarrow$ Transform the data to a 2D picture
17: Export O_i to a TIF format file
18: **end for**
19: **return** O_i

G. Algorithm

Algorithm 1 was designed to identify and filter areas that were previously marked, fit and tune a machine learning model, predict unlabelled data, and segment the results.

Algorithm 1 contains a training part where data is read as an array of attributes or features, processed by the classifier afterwards. In Step 3, sample pictures G are transformed from their RGB colour model to hue, saturation, value (HSV) colour model to obtain the feature array D. Next, in Step 5 a group of 2D filters are used on G, whose resulted pictures are added to D, subsequently. From Equations 2 and 3, these filters estimate the variance from a subset of pixels held in a kernel.

$$X = \frac{1}{w^2} \begin{bmatrix} 1 & 1 & \cdots & 1 \\ 1 & 1 & \cdots & 1 \\ \vdots & \vdots & \ddots & \vdots \\ 1 & 1 & \cdots & 1 \end{bmatrix} \tag{2}$$

$$s^2 = E[X^2] - E[X]^2 \tag{3}$$

where X is the filter kernel, w is the size, and s^2 is the variance, described as the subtraction between the mean of square and the square of mean. For this case study, the array D comprises 10 parts listed: hue; saturation; value; 2D filters on hue, with w equals 3 and 15; on saturation, with w equals 3 and 15; and on G_i in grayscale, with w equals 3, 7 and 15. Succeeding, by using Equation 4 in Step 6, labelled pixels are filtered employing the masks H.

$$D_j = \begin{cases} [G_i(x,y),\ H_i(x,y)] & \text{if } H_i(x,y) \neq 0 \\ \text{null} & \text{otherwise} \end{cases} \tag{4}$$

where D_j is the generated 2D array, $G_i(x,y)$ is the sample picture and $H_i(x,y)$ is the labelled counterpart of G_i in the position (x,y). The samples were split arbitrarily into training (D_T) and testing (D_E) arrays at 75% and 25% respectively. In Step 9, the arrays are processed to a XGBoost classifier [35], optimised for excellent performance and huge tree structures. In step 11, a grid search is performed to tune classifier's hyper-parameters like the learning rate, the number of estimators and maximum depth. In this circumstance, the optimal values without causing over-fitting are:

$$\text{learning rate} = 0.1,\ \text{estimators} = 100,\ \text{maximum depth} = 3$$

where "learning rate" is the size of each boosting step, "estimators" is the number of trees and "maximum depth" is the highest depth per tree which determines model's complexity. From Steps 13 to 17, all the orthomosaic patches are processed utilising the fit classifier, employing the same data transformations explained above. Eventually, pixels are repainted using distinct colours and the entire picture exported in TIF format.

III. Results and Discussion

A sum of 85657 labelled pixels from the photo interpretation task was assessed using D_E. The confusion matrix of the classifier, as well as its classification report, are shown in Table I.

From the table, precision is defined as the proportion of labelled instances as true positives (TP) and the sum of TP and false positives (FP); recall as the proportion of TP and the sum of TP and false negatives (FN); f-score is the mean of precision and recall; and support is the number of processed pixels per group. Here, while precision errors refer to misleading results by classifying pixels in wrong classes, recall errors represent the extent of an incomplete class detection. In sum, virtually all the classes showed accurate classification results. Misclassification records of buffel grass and spinifex were considerably small. For the former, for example, precision and recall errors were of 1.92% and 1.40%, and spinifex error rates of 2.23% and 3.11%, respectively. Furthermore, decomposed vegetation (2.88% and 2.69%) and spinifex errors (0.98% and 1.05%) happened because of multiple instances the weed was found in senescence conditions. In contrast, bushes error reports were higher, with pixels classified incorrectly as buffel grass (3.81% and 13.59%) and spinifex (0.49% and 1.74%). Conclusively, Algorithm 1 has overall rates of 97% and 95.76%. However, certain bushes were misclassified as buffel grass, considering a recall value of 84.15%. Holding an equivalent significance of precision and recall in the research, the overall classification rate is 96.54%. Examples of the segmentation process are illustrated in Figure 3.

As shown in Figures 3a and 3c, samples of invasive grasses and other vegetation are segmented at diverse spatial densities and illumination conditions. Figures 3b and 3d depict the processed segmentation. Reviewing the classification report from Table I, the framework offers accurate mapping outputs

TABLE I
CONFUSION MATRIX AND CLASSIFICATION REPORT

	Predicted	Buffel	Soil	Bushes	Shadow	Dry Veg.	Spinifex	Precision (%)	Recall (%)	F-Score (%)	Support
Labelled	Buffel	**25256**	17	156	0	4	362	95.60	97.91	96.75	25795
	Soil	15	**25196**	1	0	1	0	99.88	99.93	99.90	25213
	Bushes	632	1	**3913**	2	21	81	95.53	84.15	89.84	4650
	Shadow	0	1	0	**7729**	0	0	99.95	99.99	99.97	7730
	Dry Veg.	8	10	6	2	**5734**	159	96.68	96.87	96.78	5919
	Spinifex	508	2	20	0	171	**15649**	96.30	95.71	96.00	16350
							Mean	**97.32**	**95.76**	**96.54**	$\sum$= **85657**

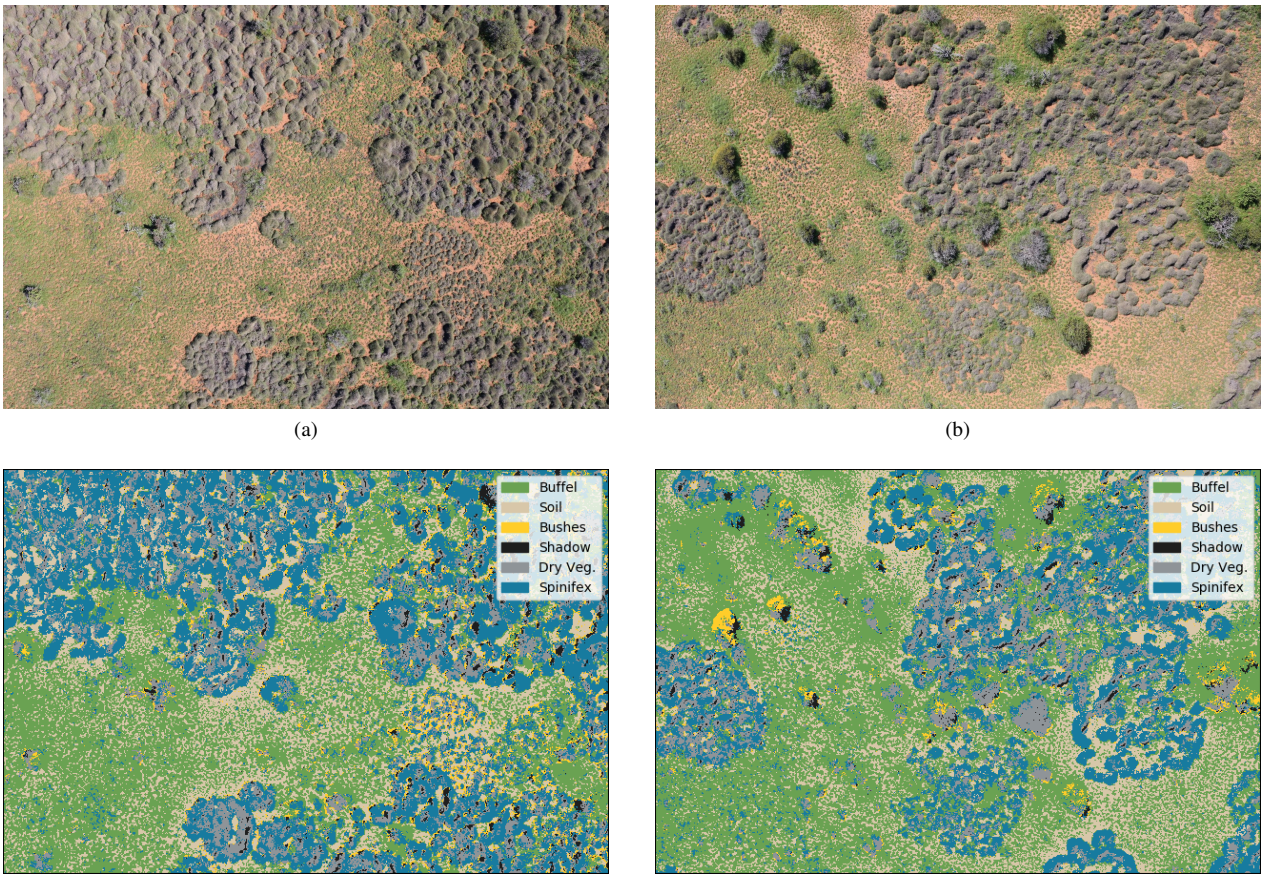

(a) (b) (c) (d)

Fig. 3. Final outputs of Algorithm 1. (a) (b) Orthorectified images. (c) (d) Classification and segmentation outputs.

for buffel grass, soil, spinifex and shadows. Still, bushes classification is variable in some photos, perceived in various cases as picture noise.

Proportions of misclassifications for buffel grass and spinifex are virtually negligible and tentatively caused by human errors during the photo interpretation phase. From a biosecurity and monitoring perspective, the presented approach provides essential data like the spread trends of invasive grasses, their proportion rates in arid lands, forecasts in the short and mid-term, among others.

This investigation shares a reliable assessment tool by the integration of UAVs and machine learning classifiers for invasive grasses, weeds and vegetation. Regarding the detection and mapping of invasive grasses in arid lands, this work satisfies the requirements for accurate and efficient surveillance solutions utilising high-resolution RGB pictures and pixel-wise classification solely without the need for multi- or hyperspectral data.

In this case study, the vegetation presented small size changes, occlusion, background clutter, and viewpoint changes, representing, possibly, an advantage in the complexity of the issue. Low GSD values for image processing confirms how improvements in sensing abilities of UAVs and their sensing equipment, opposite to satellite and manned aircraft for invasive grass surveys. Further investigations should evaluate the effectiveness of both unsupervised and supervised

models to label vegetation and invasive grass contours precisely. Also, particular areas should be better developed for real-time purposes.

IV. Conclusion

This work presents a mixed methodology to detect and segment vegetation and invasive grasses in arid lands. The classification algorithm was illustrated by achieving detection reports of 96.75% for individual identification of buffel grass and 96.00% for spinifex, and an overall detection rate of 96.54%. Invasive grasses and vegetation were captured at GSD values up to 1.015 cm/pixel and recognised at various spatial densities, confirming the reliability of UAS for the detection of invasive grasses at early stages. Further research should be concentrated on integrating vegetation labelling using supervised and unsupervised models and reduce processing times during the training and prediction stages.

Acknowledgment

This work was funded by the Plant Biosecurity Cooperative Research Centre (PBCRC) 2164 project, Agriculture Victoria Research and Queensland University of Technology (QUT). The authors would like to acknowledge Derek Sandow and WA Parks and Wildlife Service for the logistic support and permits to access the survey areas at Cape Range National Park. The authors would like to acknowledge Eduard Puig-Garcia for his contributions in co-planning the experimentation phase. The authors gratefully acknowledge the support of the QUT Research Engineering Facility (REF) Operations Team (Dirk Lessner, Dean Gilligan, Gavin Broadbent and Dr Dmitry Bratanov) who operated the DJI S800 EVO, sensors and performed ground referencing. We thank Gavin Broadbent for 2-axis gimbal for hyperspectral camera design, manufacturing and tuning. We also acknowledge the High-Performance Computing and Research Support Group at QUT, for the computational resources and services used in this work.

References

[1] R. Godfree, J. Firn, S. Johnson, N. Knerr, J. Stol, and V. Doerr, "Why non-native grasses pose a critical emerging threat to biodiversity conservation, habitat connectivity and agricultural production in multifunctional rural landscapes," *Landscape Ecology*, vol. 32, no. 6, pp. 1219–1242, may 2017. [Online]. Available: http://link.springer.com/10.1007/s10980-017-0516-9

[2] C. Schlesinger, S. White, and S. Muldoon, "Spatial pattern and severity of fire in areas with and without buffel grass (Cenchrus ciliaris) and effects on native vegetation in central Australia," *Austral Ecology*, vol. 38, no. 7, pp. 831–840, nov 2013. [Online]. Available: http://doi.wiley.com/10.1111/aec.12039

[3] R. J. Fensham, J. Wang, and C. Kilgour, "The relative impacts of grazing, fire and invasion by buffel grass (Cenchrus ciliaris) on the floristic composition of a rangeland savanna ecosystem," *The Rangeland Journal*, vol. 37, no. 3, p. 227, 2015. [Online]. Available: http://www.publish.csiro.au/?paper=RJ14097

[4] A. C. Grice, "The impacts of invasive plant species on the biodiversity of Australian rangelands," *The Rangeland Journal*, vol. 28, no. 1, p. 27, may 2006. [Online]. Available: http://www.publish.csiro.au/?paper=RJ06014

[5] V. Marshall, M. Lewis, and B. Ostendorf, "Buffel grass (Cenchrus ciliaris) as an invader and threat to biodiversity in arid environments: A review," *Journal of Arid Environments*, vol. 78, pp. 1–12, mar 2012. [Online]. Available: http://linkinghub.elsevier.com/retrieve/pii/S0140196311003399

[6] S. Bonney, A. Andersen, and C. Schlesinger, "Biodiversity impacts of an invasive grass: ant community responses to Cenchrus ciliaris in arid Australia," *Biological Invasions*, vol. 19, no. 1, pp. 57–72, jan 2017. [Online]. Available: http://link.springer.com/10.1007/s10530-016-1263-6

[7] J. Jackson, "Is there a relationship between herbaceous species richness and buffel grass (Cenchrus ciliaris)?" *Austral Ecology*, vol. 30, no. 5, pp. 505–517, aug 2005. [Online]. Available: http://doi.wiley.com/10.1111/j.1442-9993.2005.01465.x

[8] T. G. Martin, H. Murphy, A. Liedloff, C. Thomas, I. Chadès, G. Cook, R. Fensham, J. McIvor, and R. D. van Klinken, "Buffel grass and climate change: a framework for projecting invasive species distributions when data are scarce," *Biological Invasions*, vol. 17, no. 11, pp. 3197–3210, nov 2015. [Online]. Available: http://link.springer.com/10.1007/s10530-015-0945-9

[9] G. Miller, M. Friedel, P. Adam, and V. Chewings, "Ecological impacts of buffel grass (Cenchrus ciliaris L.) invasion in central Australia does field evidence support a fire-invasion feedback?" *The Rangeland Journal*, vol. 32, no. 4, p. 353, 2010. [Online]. Available: http://www.publish.csiro.au/?paper=RJ09076

[10] A. Smyth, M. Friedel, and C. O'Malley, "The influence of buffel grass (Cenchrus ciliaris) on biodiversity in an arid Australian landscape," *The Rangeland Journal*, vol. 31, no. 3, p. 307, 2009. [Online]. Available: http://www.publish.csiro.au/?paper=RJ08026

[11] L. Gonzalez, E. Whitney, K. Srinivas, and J. Periaux, "Multidisciplinary aircraft design and optimisation using a robust evolutionary technique with variable fidelity models," vol. 6, 2004, pp. 3610–3624. [Online]. Available: https://www.scopus.com/inward/record.uri?eid=2-s2.0-20344385265&partnerID=40&md5=06fc8c29f930c3d23c096ffd18eb6718

[12] E. Whitney, L. Gonzalez, J. Periaux, M. Sefrioui, and K. Srinivas, "A robust evolutionary technique for inverse aerodynamic design," 2004, p. 2. [Online]. Available: https://www.scopus.com/inward/record.uri?eid=2-s2.0-84893517420&partnerID=40&md5=44db380d2ce752df1f55fd639003bbf6

[13] A. Mancini, E. Frontoni, P. Zingaretti, and S. Longhi, "High-resolution mapping of river and estuary areas by using unmanned aerial and surface platforms," in *2015 International Conference on Unmanned Aircraft Systems (ICUAS)*, June 2015, pp. 534–542.

[14] A. Mancini, E. Frontoni, and P. Zingaretti, "A multi/hyper-spectral imaging system for land use/land cover using unmanned aerial systems," in *2016 International Conference on Unmanned Aircraft Systems (ICUAS)*, June 2016, pp. 1148–1155.

[15] L. Gonzalez, G. Montes, E. Puig, S. Johnson, K. Mengersen, and K. Gaston, "Unmanned Aerial Vehicles (UAVs) and Artificial Intelligence Revolutionizing Wildlife Monitoring and Conservation," *Sensors*, vol. 16, no. 1, p. 97, jan 2016. [Online]. Available: http://www.mdpi.com/1424-8220/16/1/97

[16] J. Chahl, "Unmanned aerial systems (uas) research opportunities," *Aerospace*, vol. 2, no. 2, pp. 189–202, 2015. [Online]. Available: http://www.mdpi.com/2226-4310/2/2/189

[17] R. S. Allison, J. M. Johnston, G. Craig, and S. Jennings, "Airborne optical and thermal remote sensing for wildfire detection and monitoring," *Sensors*, vol. 16, no. 8, 2016. [Online]. Available: http://www.mdpi.com/1424-8220/16/8/1310

[18] J. E. Thomas, T. A. Wood, M. L. Gullino, and G. Ortu, *Diagnostic Tools for Plant Biosecurity*. Cham: Springer International Publishing, 2017, pp. 209–226. [Online]. Available: https://doi.org/10.1007/978-3-319-46897-6_10

[19] A. D. Olsson, W. J. van Leeuwen, and S. E. Marsh, "Feasibility of Invasive Grass Detection in a Desertscrub Community Using Hyperspectral Field Measurements and Landsat TM Imagery," *Remote Sensing*, vol. 3, no. 12, pp. 2283–2304, oct 2011. [Online]. Available: http://www.mdpi.com/2072-4292/3/10/2283/

[20] T. Alexandridis, A. A. Tamouridou, X. E. Pantazi, A. Lagopodi, J. Kashefi, G. Ovakoglou, V. Polychronos, and D. Moshou, "Novelty Detection Classifiers in Weed Mapping: Silybum marianum Detection on UAV Multispectral Images," *Sensors*, vol. 17, no. 9, p. 2007, sep 2017. [Online]. Available: http://www.mdpi.com/1424-8220/17/9/2007

[21] T. Blaschke, G. J. Hay, M. Kelly, S. Lang, P. Hofmann, E. Addink, R. Queiroz Feitosa, F. van der Meer, H. van der Werff, F. van Coillie, and D. Tiede, "Geographic Object-Based Image Analysis - Towards a new paradigm," *ISPRS Journal of Photogrammetry and Remote Sensing*, vol. 87, pp. 180–191, 2014.

[22] J. Torres-Snchez, F. Lpez-Granados, and J. Pea, "An automatic object-based method for optimal thresholding in uav images: Application for vegetation detection in herbaceous crops," *Computers and Electronics in Agriculture*, vol. 114, no. Supplement C, pp. 43 – 52, 2015. [Online]. Available: http://www.sciencedirect.com/science/article/pii/S0168169915001052

[23] C. Yuan, Z. Liu, and Y. Zhang, "Fire detection using infrared images for uav-based forest fire surveillance," in *2017 International Conference on Unmanned Aircraft Systems (ICUAS)*, June 2017, pp. 567–572.

[24] V. M. Marshall, M. M. Lewis, and B. Ostendorf, "Detecting new Buffel grass infestations in Australian arid lands: evaluation of methods using high-resolution multispectral imagery and aerial photography," *Environmental Monitoring and Assessment*, vol. 186, no. 3, pp. 1689–1703, mar 2014. [Online]. Available: http://link.springer.com/10.1007/s10661-013-3486-7

[25] D. Ashourloo, H. Aghighi, A. A. Matkan, M. R. Mobasheri, and A. M. Rad, "An Investigation Into Machine Learning Regression Techniques for the Leaf Rust Disease Detection Using Hyperspectral Measurement," *IEEE Journal of Selected Topics in Applied Earth Observations and Remote Sensing*, vol. 9, no. 9, pp. 4344–4351, sep 2016. [Online]. Available: http://ieeexplore.ieee.org/document/7533506/

[26] T. Robinson, G. Wardell-Johnson, G. Pracilio, C. Brown, R. Corner, and R. van Klinken, "Testing the discrimination and detection limits of WorldView-2 imagery on a challenging invasive plant target," *International Journal of Applied Earth Observation and Geoinformation*, vol. 44, pp. 23–30, feb 2016. [Online]. Available: http://www.sciencedirect.com/science/article/pii/S0303243415300088http://linkinghub.elsevier.com/retrieve/pii/S0303243415300088

[27] F. Lin, D. Zhang, Y. Huang, X. Wang, and X. Chen, "Detection of Corn and Weed Species by the Combination of Spectral, Shape and Textural Features," *Sustainability*, vol. 9, no. 8, p. 1335, aug 2017. [Online]. Available: http://www.mdpi.com/2071-1050/9/8/1335

[28] O. Schmittmann and P. Lammers, "A True-Color Sensor and Suitable Evaluation Algorithm for Plant Recognition," *Sensors*, vol. 17, no. 8, p. 1823, aug 2017. [Online]. Available: http://www.mdpi.com/1424-8220/17/8/1823

[29] Plant Biosecurity Cooperative Research Centre, "Biosecurity built on science," http://www.webcitation.org/6xPa92DuM, 2016, (Archived on 22-Feb-2018).

[30] J. Sandino, F. Gonzalez, K. Mengersen, and K. J. Gaston, "Uavs and machine learning revolutionising invasive grass and vegetation surveys in remote arid lands," *Sensors*, vol. 18, no. 2, 2018. [Online]. Available: http://www.mdpi.com/1424-8220/18/2/605

[31] F. Gonzalez and E. Puig Garcia, "Assessment of invasive grasses using unmanned aerial vehicles: A machine learning approach," vol. 7, no. 3, 2017. [Online]. Available: https://www.omicsonline.org/conference-proceedings/2155-952X-C1-076-010.pdf

[32] J. Sandino, A. Wooler, and F. Gonzalez, "Towards the automatic detection of pre-existing termite mounds through uas and hyperspectral imagery," *Sensors*, vol. 17, no. 10, 2017. [Online]. Available: http://www.mdpi.com/1424-8220/17/10/2196

[33] Bureau of Meteorology, "Learmonth, WA - July 2016 - Daily Weather Observations," 2016. [Online]. Available: http://www.bom.gov.au/climate/dwo/201607/html/IDCJDW6073.201607.shtml

[34] F. Pedregosa, G. Varoquaux, A. Gramfort, V. Michel, B. Thirion, O. Grisel, M. Blondel, P. Prettenhofer, R. Weiss, V. Dubourg, J. Vanderplas, A. Passos, D. Cournapeau, M. Brucher, M. Perrot, and E. Duchesnay, "Scikit-learn: Machine learning in Python," *Journal of Machine Learning Research*, vol. 12, pp. 2825–2830, 2011.

[35] T. Chen and C. Guestrin, "Xgboost: A scalable tree boosting system," in *Proceedings of the 22Nd ACM SIGKDD International Conference on Knowledge Discovery and Data Mining*, ser. KDD '16. New York, NY, USA: ACM, 2016, pp. 785–794. [Online]. Available: http://doi.acm.org/10.1145/2939672.2939785

[36] J. D. Hunter, "Matplotlib: A 2d graphics environment," *Computing In Science & Engineering*, vol. 9, no. 3, pp. 90–95, 2007.

[37] G. Bradski, "The OpenCV library," *Dr. Dobb's Journal of Software Tools*, 2000.